3-15-2015

Asymmetric Kelvin-Helmholtz Propagation at Saturn's Dayside Magnetopause

X. Ma
University of Alaska, Fairbanks, max@erau.edu

B. Stauffer
University of Alaska, Fairbanks

P. A. Delamere
University of Alaska, Fairbanks

A. Otto
University of Alaska, Fairbanks

Scholarly Commons Citation

Ma, X., Stauffer, B., Delamere, P. A., & Otto, A. (2015). Asymmetric Kelvin-Helmholtz Propagation at Saturn's Dayside Magnetopause. *Journal of Geophysical Research: Space Physics, 120*(3). https://doi.org/10.1002/2014JA020746

AGU PUBLICATIONS

JGR

Journal of Geophysical Research: Space Physics

RESEARCH ARTICLE

10.1002/2014JA020746

Key Points:
- Saturn's magnetopause is asymmetric for KH onset condition
- On the dawnside, fast-growing KHI generates broad boundary
- On the duskside, slow-growing KHI are likely observed by satellite

Correspondence to:
X. Ma,
xma2@alaska.edu

Citation:
Ma, X., B. Stauffer, P. A. Delamere, and A. Otto (2015), Asymmetric Kelvin-Helmholtz propagation at Saturn's dayside magnetopause, *J. Geophys. Res. Space Physics*, *120*, 1867–1875, doi:10.1002/2014JA020746.

Received 17 OCT 2014
Accepted 17 FEB 2015
Accepted article online 19 FEB 2015
Published online 19 MAR 2015

Asymmetric Kelvin-Helmholtz propagation at Saturn's dayside magnetopause

X. Ma[1], B. Stauffer[1], P. A. Delamere[1], and A. Otto[1]

[1]Geophysical Institute, University of Alaska Fairbanks, Fairbanks, Alaska, USA

Abstract At Saturn's magnetopause, the shear flows are maximized (minimized) in the prenoon (postnoon) sector due to the rapid planetary rotation and the corotating magnetodisc. As such, the prenoon sector is expected to be more Kelvin-Helmholtz (KH) unstable than the postnoon sector; however, in situ Cassini data analyses showed that the evidence of KH activity favors the postnoon sector. In this study, we use a two-dimensional MHD simulation to demonstrate that fast-growing KH modes strongly deform and diffuse the boundary layer on a time scale of a few minutes in the prenoon sector. Therefore, the KH observational signature is difficult to identify by spacecraft in the diffused boundary layer. KH vortices originating in the subsolar region (roughly from 10 to 14 local times) are transported to the postnoon sector and the wavelength is enlarged due to the gradient of shear flow, which is a plausible reason why KH events are more often observed in the postnoon sector. The prediction of the local boundary normal direction distribution as a function of spacecraft inward/outward crossing in the postnoon sector suggested by our simulation is qualitatively consistent with Cassini in situ observational results. We also discuss the impact of this dawn-dusk asymmetric Kelvin-Helmholtz evolution on magnetic reconnection at Saturn's magnetopause boundary.

1. Introduction

Saturn's magnetopause boundary is the interface between the solar wind and the magnetosphere, facilitating the transport of mass, momentum, energy, and magnetic flux. Key processes mediating the solar wind interaction include the shear flow-driven Kelvin-Helmholtz (KH) instability and/or magnetic reconnection. Observational evidence (Cassini data analysis) indicates that KH is operating [*Masters et al.*, 2009, 2010, 2012a; *Delamere et al.*, 2011, 2013; *Wilson et al.*, 2012]. However, to date, there is little in situ evidence to support a strong reconnection-mediated interaction. *McAndrews et al.* [2008] and *Badman et al.* [2013] found indications of reconnection based on heating of the plasma and anisotropic electron populations [*Fuselier et al.*, 2014]. Nevertheless, *Lai et al.* [2012] searched the magnetopause at local times (LT) from 10 to 14 but found no evidence of flux transfer events. *Masters et al.* [2012b] suggested that reconnection at Saturn may be suppressed by large plasma β gradient conditions and this conclusion was supported by *Desroche et al.* [2013].

On the other hand, *Badman et al.* [2005] argued that reconnection must occur. During the January 2004 Cassini-Hubble Space Telescope campaign, the open flux content of the southern polar region, measured using the poleward boundary of the main oval of emissions, varied between 15 and 50 GWb, with dramatic tail reconnection occurring with high solar wind dynamic pressure. In the absence of compelling in situ evidence for magnetic reconnection, there has been considerable effort recently to identify reconnection signatures in the aurora. *Radioti et al.* [2011, 2013] and *Badman et al.* [2013] have suggested that bifurcations of the dayside main auroral ring may be signatures of consecutive reconnection events at Saturn's magnetopause.

Saturn's magnetopause boundary is expected to be KH unstable due, in part, to the rapid planetary rotation (~10 h period) and the corotating magnetodisc. The KH instability onset condition is given by [*Chandrasekhar*, 1961]

$$\left[\mathbf{k}\cdot\left(\mathbf{V}_{\mathrm{MSP}}-\mathbf{V}_{\mathrm{MSH}}\right)\right]^2 > \frac{\rho_{\mathrm{MSP}}+\rho_{\mathrm{MSH}}}{\mu_0\rho_{\mathrm{MSP}}\rho_{\mathrm{MSH}}}\left[\left(\mathbf{k}\cdot\mathbf{B}_{\mathrm{MSP}}\right)^2+\left(\mathbf{k}\cdot\mathbf{B}_{\mathrm{MSH}}\right)^2\right], \tag{1}$$

and a KH wave propagates at a speed of

$$\mathbf{V}_{\mathrm{KH}}=\frac{\rho_{\mathrm{MSP}}\mathbf{V}_{\mathrm{MSP}}+\rho_{\mathrm{MSH}}\mathbf{V}_{\mathrm{MSH}}}{\rho_{\mathrm{MSP}}+\rho_{\mathrm{MSH}}}. \tag{2}$$

Here MSP and MSH refer to the magnetosheath and magnetosphere, respectively; **V**, **B**, **k**, and ρ denote velocity, magnetic field, KH wave number, and density, respectively; and μ_0 is the vacuum permeability. Equation (1) indicates that large shear increases the Kelvin-Helmholtz instability (KHI) rate, and the presence of magnetic field components along the shear flow direction stabilizes the KHI mode. Equation (2) implies that the KH wave will be stationary if the net momentum is small (i.e., $\rho_{MSP}\mathbf{V}_{MSP} \approx -\rho_{MSH}\mathbf{V}_{MSH}$). *Miura and Pritchett* [1982] suggested that the fastest growing modes occur for $2ka \approx 0.5 \sim 1.0$, where a is the half width of the shear flow layer.

When considering physical processes at Saturn's magnetopause boundary, it is critical to understand the interaction between KH and reconnection. In two-dimensional geometry, reconnection and KH are mutually exclusive with reconnection requiring sub-Alfvénic flows along the reconnecting components and KH requiring super-Alfvénic shear flow. However, in a full three-dimensional geometry, *Ma et al.* [2014a, 2014b] have recently demonstrated that reconnection can trigger KH and conversely KH can trigger reconnection. If we assume that KH is the primary driver of magnetic reconnection, then following *Ma et al.* [2014a], reconnection is triggered along the "spine" connecting neighboring vortices. While adjacent vortices execute a nonlinear rollup, the preexisting magnetopause current sheet is thinned, allowing reconnection to operate [*Otto and Fairfield*, 2000].

To address the issue of the interaction between KH and reconnection at Saturn, it is important to understand potential dawn/dusk asymmetries in the evolution of KH vortices. The shear flows are maximized in the prenoon sector due to the opposing sheath and magnetospheric flows. In the postnoon sector, the flows are both directed tailward and KH is more likely to be stabilized. However, contrary to expectation, *Masters et al.* [2012a] and *Delamere et al.* [2013] showed that evidence of KH activity favors the postnoon sector.

We address the asymmetric development of the KH instability at Saturn's dayside magnetopause boundary by conducting high-resolution two-dimensional MHD simulations that include an asymmetric shear flow through the subsolar region (roughly from 10 LT to 14 LT). Previous global-scale MHD simulations [e.g., *Walker et al.*, 2011] showed a relatively symmetric development of KH vortices along the terminator flanks, but these simulations did not resolve the KH growth in the subsolar region where the boundary is still expected to be KH unstable [*Desroche et al.*, 2013]. We show indeed that vortices starting in the subsolar region propagate through noon and toward the dusk flank. At roughly to 10 LT, the vortices are stationary due to balanced momentum in the sheath and magnetosphere. However, fast-growing KH vortices can diffuse the boundary in a short period of time; consequently, KH evidences are unlikely to be observed in this region. At $<$ 10 LT the vortices propagate tailward. Comparing with boundary normal analysis of Cassini MAG data [*Dougherty et al.*, 2004], we find that the magnetopause boundary crossing is consistent with the asymmetric development of KH vortices in our numerical simulations. Implications for KH-triggered magnetic reconnection will be discussed.

2. Asymmetric Kelvin-Helmholtz Simulations

To fully self-consistently resolve the evolution of KH waves along Saturn's dayside magnetopause, a high spatial resolution and low numerical dissipation global model is required, which is computationally expensive. However, the key physical process can be demonstrated by using part of a two-cell convection configuration to mimic the dayside magnetosheath flow, as is illustrated in Figure 1 (top). The x direction represents the tangential direction from the duskside to the dawnside, which is approximately the negative azimuthal direction; the y direction is the normal direction from the magnetosphere to the magnetosheath; and the z direction points to the north. Figure 1 (top) presents the magnetic B_z component (color index) and the in-plane bulk velocity (blue arrows) at early time ($t = 50$) in our simulation, which shows an asymmetric shear flow and three small KH waves close to the subsolar point ($x = 0$). Thus, the right and left part of simulation domain represents the prenoon and postnoon sector, respectively; and $x = 0$ is the subsolar point. The magnetospheric flow is consistent with corotation of the magnetodisc.

In this study, the full set of two-dimensional MHD equations are normalized to the typical values (Table 1) and solved by the leapfrog method [*Otto*, 1990]. Low numerical dissipation is an advantage of this code, which has been tested in the Geospace Environment Modeling magnetic reconnection challenge [*Otto*, 2001]. The numerical simulation is carried out in a rectangular box with $|x| \le L_x = 250$ and $|y| \le L_y = 30$, which is resolved by using 1253×503 grid points with a uniform grid. In physical units, this simulation domain

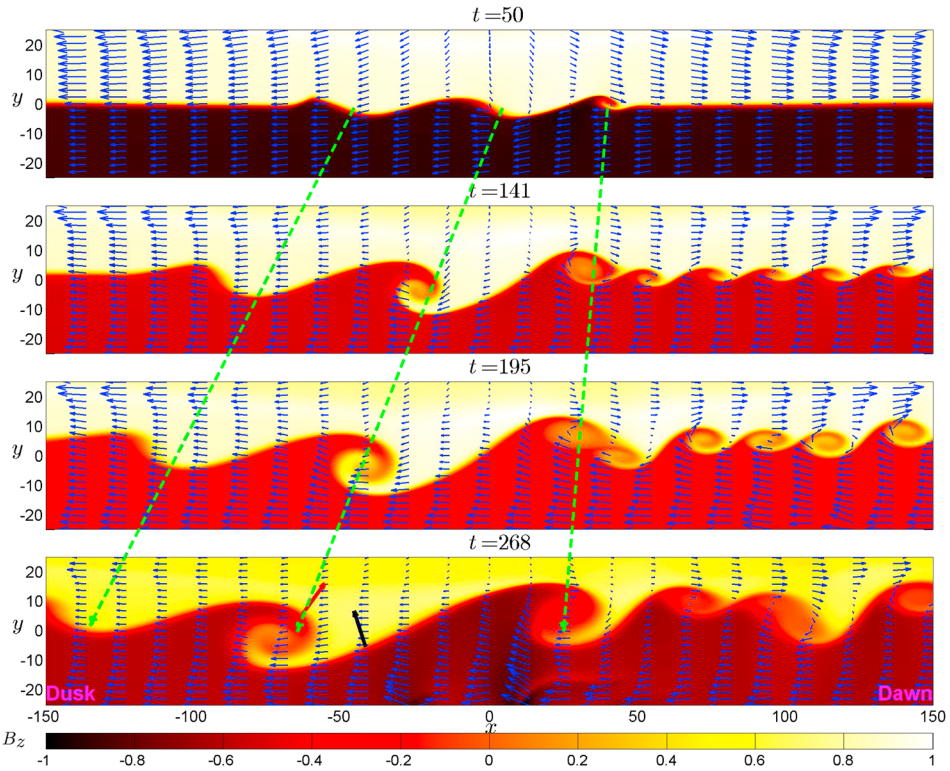

Figure 1. (from top to bottom) MHD simulation of KH waves propagating along the Saturn's magnetopause boundary at $t = 50$, 141, 195, and 268, respectively. The color index presents the magnetic B_z component, and blue arrows are the bulk velocity in the xy plane. The black and red arrows represent the local normal directions in the spine region and vortex region, respectively.

roughly represents a range from 9 LT to 15 LT with a resolution of 1200 km for a magnetospheric size of $\sim 22\,R_S$ under typical solar wind conditions [*Kanani et al.*, 2010].

The initial two-cell flow is given by $\mathbf{V} = \nabla\Phi(x, y) \times \hat{\mathbf{e}}_z$, where

$$\Phi = -\frac{1}{2}\left\{ V_{\mathrm{MSH}}\left[y - y_0 + \ln\frac{\cosh(y)}{\cosh(y_0)} \right] \tanh\left(\frac{x}{D_x}\right) + V_{\mathrm{MSP}}\left[y - y_0 - \ln\frac{\cosh(y)}{\cosh(y_0)} \right] \right\} \tag{3}$$

is the stream function. Here $V_{\mathrm{MSH}} = 1$ and $V_{\mathrm{MSP}} = -0.5$ represent the azimuthal speed at the terminator on the magnetosheath and magnetospheric side, respectively. The parameter, D_x, determines the gradient of the magnetosheath flow, which depends on specific solar wind conditions. However, due to the solar wind compression, this shear flow gradient only spans a small fraction of the flat low-latitude dayside magnetopause. In our simulation, $D_x = 80 \approx 4\,R_S$ is equivalent to 10° [*Desroche et al.*, 2013] at low-latitude dayside magnetopause for a magnetospheric size of $22\,R_S$. Note that the change of D_x can affect the growth and size of KH wave. However, our major conclusion is, in principle, only based on the direction of the magnetosheath and the magnetopause flow, which is insensitive to the D_x. To approach the static state, we require the divergence of flux, $\nabla \cdot (\rho\mathbf{V})$ to vanish, which yields a uniform density. The initial magnetic field is chosen as $\mathbf{B} = \frac{1}{2}B_{x0}\left[1 + \tanh(y)\right]\hat{\mathbf{e}}_x + B_{z0}\tanh(y)\hat{\mathbf{e}}_z$. In two dimensions, the magnetic B_z component is convected by the plasma, which is equivalent to an additional pressure and does not play an important role for the dynamic process. Thus, the antisymmetric B_z component is applied to identify the magnetosheath and magnetosphere. Note that the system is hydrodynamically unstable. Therefore, any perturbation

Table 1. Normalized Physical Quantities and Their Values

Normalized Physical Quantities	Values
Length scales, L_0	$0.05\,R_S \approx 3000$ km
Number density, n_0	0.1 cm^{-3}
Magnetic field, B_0	5.8 nT
Alfvén velocity, $V_0 = B_0/\sqrt{\mu_0 n_0 m_0}$	400 km s^{-1}

can cause strong interchange instability. In realistic three-dimensional magnetopause, such instability is suppressed by the magnetic tension. In this numerical simulation, a small $B_x = 0.1$ component is added to mimic this three-dimensional stability effect. To reduce the pileup of magnetic flux by the inflow solar wind (V_y), we only add this B_x component on the magnetospheric side. The thermal pressure is chosen to balance the magnetic pressure, that is, $p + B^2 = 1.26$, and the reasons are as follows. We note that this initial condition is not a steady state, and it is questionable whether a static state solution exists to satisfy the boundary condition. However, the current configuration is locally quasi-static as long as $L_y/D_x < 1$. Besides, the net effect of the unbalanced force is to push the boundary toward the magnetosphere, which is more or less consistent with the realistic magnetopause. Furthermore, most of our conclusions are independent of motion in the normal (y) direction. Thus, we argue that although one can use a more sophisticated model to approach the realistic dayside magnetospheric boundary, our model is sufficient to characterize the basic physical process of KH instability at Saturn's magnetopause.

The quasi-static initial condition is KH unstable; therefore, KH modes can operate in the prenoon sector even without any perturbation. However, in this study, we are interested in the KH vortex propagation from the subsolar region to the postnoon sector. Thus, a localized KH type stream function $\delta\Phi = \delta V \sin\left(\pi x/l_x\right) \cosh^{-1}\left(\pi y/l_x\right) \left[\tanh\left(x + 2l_x\right) - \tanh\left(x - 2l_x\right)\right]$ is introduced as the perturbation in the subsolar region. Here $\delta V = 0.2$, and $2l_x = 40$ is the wavelength.

In this configuration, it is natural to use open boundary conditions ($\partial_n = 0$, where n is the normal direction to the boundary) at $|x| = 250$ and $y = 30$ and closed boundary conditions ($B_y = V_y = 0$) at $y = -30$. An artificial friction term [*Ma et al.*, 2014a] is applied at the boundary of $y = \pm 30$ to maintain the shear flow gradient.

The dawn-dusk asymmetric KH wave evolution is presented in Figure 1. In the prenoon sector ($x > 0$), the magnetosheath velocity is antiparallel to the magnetospheric flow. As such, the large shear flow is satisfied with the KH onset condition; however, small net momentum leads to stationary vortices (see equation (2)). The short wavelength associated with the fastest growing mode develops at that very beginning, and later longer wavelength modes are observed to become dominant. The fast-growing KH vortices rapidly mix the boundary layer in a short period of time. It is well known that typical observational signatures of KH vortices include large fluctuations of the magnetic field [*Fairfield et al.*, 2000; *Delamere et al.*, 2011], and magnetic reconnection can be driven by nonlinear KH waves [*Fairfield et al.*, 2000; *Otto and Fairfield*, 2000]. However, these signatures are only available before the KH vortex has decayed or the boundary layer has been formed. At Saturn's magnetopause, the typical magnetic field is about 5 nT, the density is about 0.1 cm^{-3}, and the plasma β is about unity, which yields to a fast mode speed $V_f = \sqrt{v_A^2 + c_s^2} \approx 652$ km/s. For a shear flow layer with a half width $a \approx 1200$ km and a total velocity jump of 600 km/s, the fastest normalized KH growth rate is about 0.15 [*Miura and Pritchett*, 1982], corresponding to the shortest linear growth time ($1/q$) of about 30 s. If the vortex structure is assumed stationary and the spacecraft crosses the boundary at 5 km/s, then the entire crossing takes about 480 s. This implies that when the spacecraft reaches the center of the boundary layer, the KH vortex has already been saturated or even decayed, and the boundary layer has formed [*Karimabadi et al.*, 2013]. As such, strong fluctuations of the magnetic azimuth component (B_ϕ) is expected to be observed. However, highly patchy reconnection is likely triggered by those multiple thin current layers [*Delamere et al.*, 2013; *Ma et al.*, 2014a] and strongly diffuse the magnetic B_ϕ component, which is a plausible reason why *Delamere et al.* [2013] found fewer KH signatures (fluctuation of B_ϕ) on the prenoon side.

In the postnoon sector ($x < 0$), the magnetosheath velocity is parallel to the magnetosphere flow. Thus, such a small shear flow configuration is indeed KH stable. However, considerable net tailward momentum carries the slowly growing KH modes from the upstream region (i.e., the prenoon side of the subsolar region). In Figure 1, the leftmost KH wave moves away from its initial location without developing into a mature vortex due to the small shear flow. The middle KH wave experienced more shear flow and grows to a fully developed vortex with a shorter duskward displacement. The initial KH vortex on the right grows even faster with little duskward displacement. Note that due to the gradient of magnetosheath flow, the increase of net tailward momentum enlarges the KH wavelength, and thereby generating a long spine region ($x \in (-75, 25)$ connecting neighboring vortices in Figure 1 (bottom)). In spite of the numerical diffusion widening the spine region current layer in our results, the real physical current layer is usually thin in the

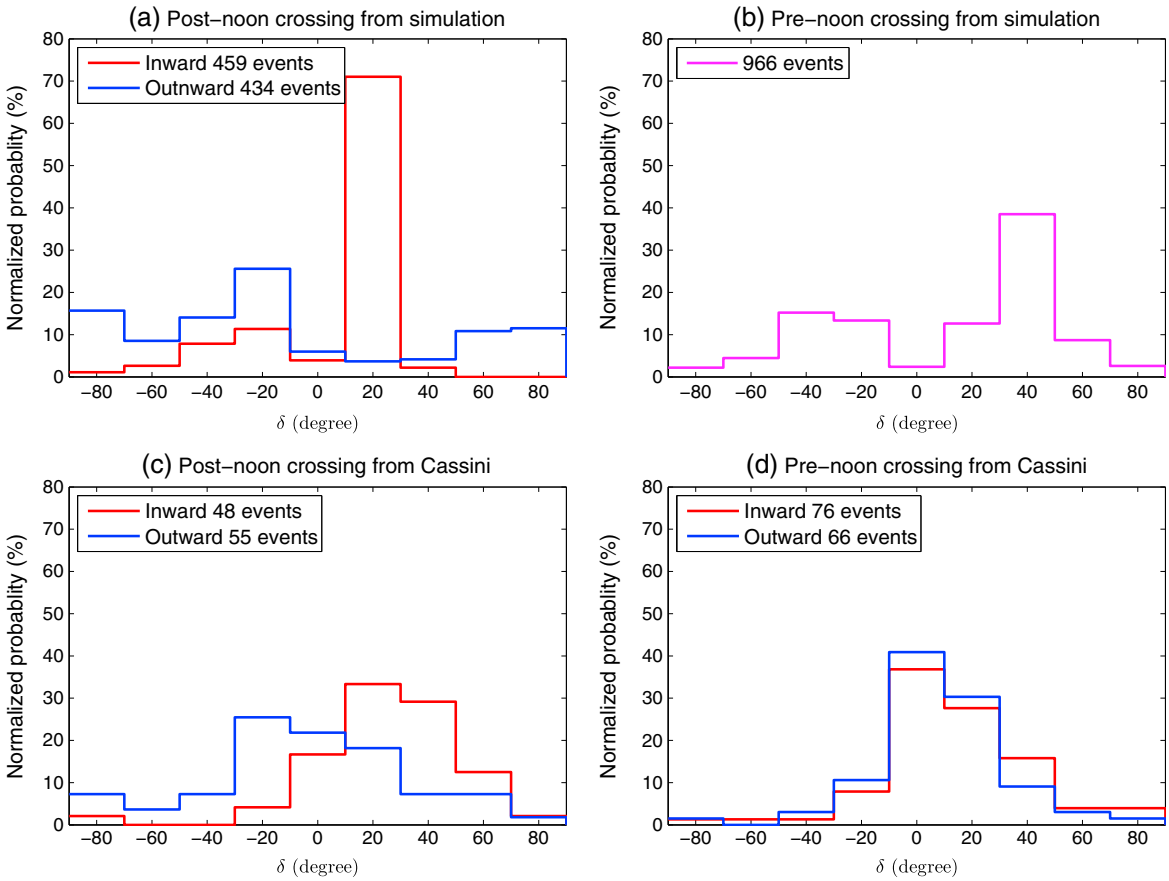

Figure 2. Normalized distribution of boundary normal direction δ for crossing events in the (a and c) postnoon and (b and d) prenoon sector based on simulation results and Cassini MAG data.

spine region, simply due to the convergence flow from both the magnetosphere and magnetosheath [*Otto and Fairfield*, 2000]. This thin spine region is susceptible to magnetic reconnection under northward interplanetary magnetic field (IMF) conditions for Saturn [*Ma et al.*, 2014a].

3. Boundary Normal Analysis

In the postnoon sector, tailward propagation of the KH waves is likely to lead to inward (MSH to MSP) crossing in the long spine region and outward (MSP to MSH) crossing at the leading edge of the KH vortex (Figure 1), assuming V_{KH} (~50–100 km/s) is much larger than the spacecraft velocity (~5 km/s). In this paper, the local normal direction, $\hat{\mathbf{n}}$, is chosen to point outward into the magnetosheath (i.e., $n_y > 0$ in simulation coordinates or $n_r > 0$ in spherical coordinates). The angle between the local normal direction and the model normal direction (e.g., the y direction in the simulation coordinates) is denoted as δ, and a positive δ indicates $\hat{\mathbf{n}}$ rotation toward the azimuthal (or the negative x) direction. Our simulation suggests that in the postnoon sector, the spine region usually has a small positive δ (black arrow in Figure 1) and the leading edge of the KH vortex has a negative δ (red arrow in Figure 1).

Here we provide an example of the δ distribution from our simulation at $t = 268$ in Figures 2a and 2b. The distribution is obtained by taking line cuts along the x direction through the simulation domain, which can be considered as satellite orbits. To achieve a sufficient sample size, we take a series of line cuts from $y = -15$ to 20 with a separation of 0.1, which covers the whole KH structure. A boundary crossing "event" is defined at a point where the magnetic B_z component is zero, and an inward (outward) crossing is $B_z > 0$ (< 0) on the left side of this point. The local normal direction is obtained from the traditional minimum variance analysis (MVA) method [*Sonnerup and Cahill*, 1967] and the Siscoe method [*Siscoe et al.*, 1968]. In this paper, we only present the results from the MVA method, because these two methods give similar results.

As we expect, Figure 2a shows a strong preference of small positive δ for 459 inward crossing events and a broad distribution of δ with a relatively smaller peak at negative values for 434 outward crossing events in the postnoon sector. In contrast, on the duskside of Earth's magnetopause, an inward crossing is likely to occur at the leading edge of the KH vortex with a positive δ and vice versa for an outward crossing, which has been widely discussed [*Fairfield et al.*, 2000; *Hwang et al.*, 2012].

As a comparison, Figure 2b shows a bimodal distribution of δ for 969 crossing events in the prenoon sector, being consistent with a boundary perturbation by KH vortices. In the prenoon sector, the low KH wave propagation speed allows spacecraft trajectory crossings through a KH vortex in any direction. Therefore, the inward (outward) crossings do not associate with the crossings in the spine region (leading edge). Furthermore, due to the rapid KH growth rates discussed above, this distribution only applies to short periods of time before the mixed boundary layer is formed. We argue that spacecraft observations of active KH growth in the prenoon sector are unlikely.

To compare with our simulation results, we conduct a statistical survey of Saturn's magnetopause boundary normal direction by using the Cassini in situ observational data. In this study, the boundary identification is based on electron temperature, ion composition, and magnetic field data which has been discussed by *Delamere et al.* [2013]. The location of crossing events are limited to the low-latitude boundary layer (i.e., within 15° latitude of the equator) in the vicinity of the subsolar region, which yields a total of 193 events in the postnoon sector (from 12 to 15 LT) from February 2007 to February 2008 and 224 events in the prenoon sector (from 9 to 12 LT) from February 2005 to March 2009. Approximately, half of these events involve a significant magnetic B_θ component jump, being suitable for the boundary normal analysis methods. For each crossing event, the time interval varies from 2 to 20 min, which is determined case by case. The robustness of our results are confirmed by the consistency of the results from different boundary normal analysis methods (i.e., the MVA, the Siscoe, and the constrain [*Sonnerup and Cahill*, 1968] methods). The model normal direction $\hat{\mathbf{N}}$ is given by an empirical Saturn magnetopause model [*Kanani et al.*, 2010], describing the radial distance of the magnetopause boundary as a function of the local time and the solar wind dynamic pressure, which can be determined from the Cassini location. Note that $\hat{\mathbf{N}}$ is a two-dimensional vector in the equator plane. Thus, δ is defined as the angle between $\hat{\mathbf{N}}$ and the projection of $\hat{\mathbf{n}}$ into the equator plane. Figures 2c and 2d show the normalized δ distribution based on Cassini crossing in the postnoon and prenoon sector, respectively. In the postnoon sector (Figure 2c), inward crossings show a significant preference for positive δ and outward crossings have a relatively broad distribution with a peak at negative values, being consistent with the simulation prediction. In contrast, both inward and outward crossings in the prenoon sector (Figures 2d) have a narrow distribution with a peak close to zero, indicating the lack of KH vortex perturbation, which is consistent with previous studies [*Masters et al.*, 2012a; *Delamere et al.*, 2013]. One should keep in mind that the results in Figure 2b only represent a short period of time, which are unlikely to be observed by the satellite. Therefore, the results of Figures 2c and 2d are incomparable. Due to the fast-growing KH waves in this sector forming a mixed boundary layer, we expect a lack of coherent KH vortex structures, as it is shown in Figure 2d.

4. Summary and Discussion

Kelvin-Helmholtz instability is an important process for the interaction between the solar wind and planetary magnetosphere or ionosphere (e.g., Earth [*Nykyri et al.*, 2006], Venus [*Terada et al.*, 2002, 2004], and Mercury [*Slavin et al.*, 2008]). A detail comparison of the KH instability in different planetary magnetospheres has been summarized by *Johnson et al.* [2014]. In this study, asymmetric KH wave propagation in Saturn's dayside due to the corotating magnetodisc is investigated by means of a MHD simulation. Our simple numerical model characterizes the basic dynamical processes, being qualitative consistent with the in situ observational results, which are summarized as follows.

In the prenoon sector, the KH instability can be easily driven by the large shear flow without any significant advection. The fast-growing KH modes strongly deform and diffuse to form the boundary layer on a time scale of a few minutes. As such, we rarely expect the spacecraft to encounter actively growing KH vortices.

In the postnoon sector, the small shear flow suppresses the KH mode onset condition. However, the slow-growing KH waves originating from the prenoon sector are likely to advect to the postnoon sector, which is a plausible reason for a higher frequency of KH signatures observed in the postnoon sector. The

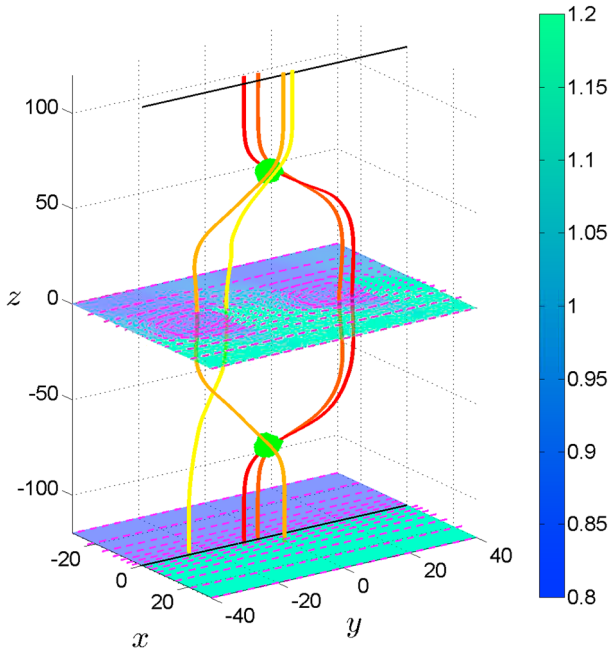

Figure 3. Selected field lines from three-dimensional KHI MHD simulation for southward IMF conditions. The color index represents the density, and red arrows are the bulk velocity in the *xy* plane. The green patches indicate the reconnection sites.

gradient of shear flow enlarges the KH wavelength when it propagates toward the tail, which lengthens the long spine region.

The boundary normal analysis shows a preference of positive δ for inward crossing and negative δ for outward crossing in the postnoon sector. If we assume that these modulations of the local boundary are caused by the KH mode, this statistical result is likely to be indicative of KH waves originating in the prenoon sector.

Note that the asymmetric propagation of KH waves is basically a two-dimensional hydrodynamic result, which is independent of the IMF orientation. The presence of the third dimension has a KH stabilizing effect. The marginal growth of the KH wave, being localized along the third dimension, requires that the kinetic energy generated by the KH mode is greater than the energy transport by Alfvén waves through Poynting flux [*Ma et al.*, 2014a]. This stabilizing effect will cause an overlong wavelength mode to break into several short-wavelength modes. However, this process does not change the sign of vorticity, $\nabla \times \mathbf{V}$, and it only occurs near the minimum shear flow region; thus, its influence on the δ distribution is minor. However, the KH mode largely modulates the local current layer, leading to two important implications for reconnection.

Based on the Parker spiral solar wind model [*Parker*, 1965], the IMF is expected to be B_y oriented (i.e., $B_x \ll B_y$) near Saturn's orbit. But a small B_z component will increase significantly for a polar-flattened magnetosphere [*Desroche et al.*, 2013]. For southward IMF conditions [*Faganello et al.*, 2012], it is clear that magnetic reconnection is switched off on the prenoon side, where the transition layer is wide and there are no antiparallel magnetic field components. In contrast, the slowly growing KH modes on the duskside are likely to locally twist magnetic flux, which leads to a pair of high-latitude magnetic reconnection regions in three dimensions (e.g., green patchy in Figure 3). This process interchanges a fraction of the flux tube and consequently transports mass and flux tube entropy. Open flux (e.g., yellow line) will be generated if the two sites of reconnection are asymmetric. A systematical study on this process will be presented in the future. We propose that this type of small-scale and intermittent reconnection contributes to a viscous-like interaction of the solar wind with the magnetosphere.

For northward IMF conditions, the large antiparallel magnetic field components with a perpendicular shear flow in three dimensions allow the KH instability and magnetic reconnection to operate simultaneously [*Ma et al.*, 2014a, 2014b]. Figure 4 is a perspective view of the selected magnetic field lines from a three-dimensional KHI MHD simulation by *Ma et al.* [2014a]. The red and black lines are the closed field lines, and the green, blue, magenta, and orange lines are the open field lines. The color index in the reference planes represents the magnetic B_z component, and black arrows indicate the plasma bulk velocity. On the prenoon side, during a short period (i.e., the longest wavelength KH mode has not diffused and formed the boundary layer), multiple current layers formed by the fast-growing KH mode generate patchy reconnection and, consequently, complex flux tubes (e.g., blue and red lines), which strongly mixes the magnetosheath and magnetospheric plasma; however, this is unlikely to contribute a large amount of open flux [*Ma et al.*, 2014a]. Nevertheless, the wide current layer formed by the KH waves eventually switches off magnetic reconnection. In contrast, the thin current layer provided by the highly stretched spine region on the

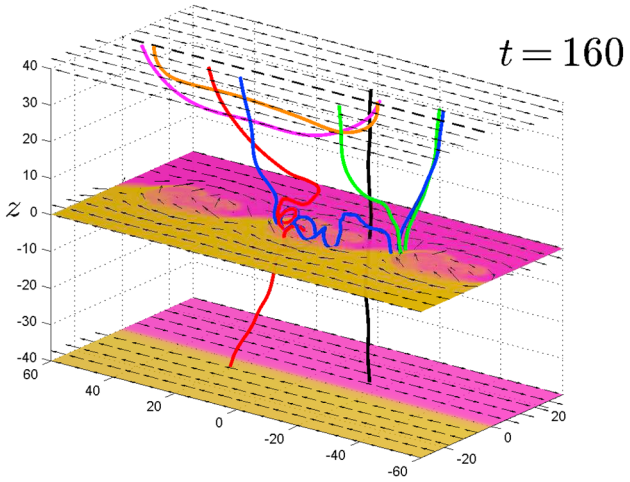

Figure 4. A perspective view of the selected magnetic field lines from three-dimensional KHI MHD simulation for northward IMF conditions [*Ma et al.*, 2014a]. The red and black lines are the closed field lines, and the green, blue, magenta, and orange lines are the open field lines. The color index in the reference planes represents the magnetic B_z component, and black arrows indicate the plasma bulk velocity.

postnoon side is the major source for simple open flux (e.g., green line). Fast jets and flux transfer event (FTE) signatures are expected to be observed away from the equatorial plane.

One should keep in mind that the interaction between the KHI and magnetic reconnection often operate at the KHI nonlinear stage, while our major conclusions are only based on the KHI onset condition, especially in the flow direction. Thus, we argue that the third dimension only has a minor influence on our conclusions. Finally, that the dense plasma of the fast corotational magnetodisc can significantly increase the Alfvén Mach number in the vicinity of equational plane. As such, both the KH mode and magnetic reconnection are switched off by the superfast-mode shear flow; therefore, fast jets and FTEs signature are likely observed at the even higher latitude [*Fukazawa et al.*, 2007a, 2007b].

Acknowledgments

The authors acknowledge support from NASA grant NNX13AF22G. We are grateful to the Cassini MAG teams for making available the data presented here. The authors are grateful to the International Space Science Institute (ISSI) for their support to the Coordinated Numerical Modeling of the Global Jovian and Saturnian Systems team. The simulation data in this paper can be accessed from the corresponding author at xma2@alaska.edu.

Michael Balikhin thanks the reviewers for their assistance in evaluating this paper.

References

Badman, S. V., E. J. Bunce, J. T. Clarke, S. W. H. Cowley, J.-C. Gérard, D. Grodent, and S. E. Milan (2005), Open flux estimates in Saturn's magnetosphere during the January 2004 Cassini-HST campaign, and implications for reconnection rates, *J. Geophys. Res.*, *110*, A11216, doi:10.1029/2005JA011240.

Badman, S. V., A. Masters, H. Hasegawa, M. Fujimoto, A. Radioti, D. Grodent, N. Sergis, M. K. Dougherty, and A. J. Coates (2013), Bursty magnetic reconnection at Saturn's magnetopause, *Geophys. Res. Lett.*, *40*, 1027–1031, doi:10.1002/grl.50199.

Chandrasekhar, S. (1961), *Hydrodynamic and Hydromagnetic Stability, The Int. Ser. of Monogr. on Phys.*, Dover, New York.

Delamere, P. A., R. J. Wilson, and A. Masters (2011), Kelvin-Helmholtz instability at Saturn's magnetopause: Hybrid simulations, *J. Geophys. Res.*, *116*, A10222, doi:10.1029/2011JA016724.

Delamere, P. A., R. J. Wilson, S. Eriksson, and F. Bagenal (2013), Magnetic signatures of Kelvin-Helmholtz vortices on Saturn's magnetopause: Global survey, *J. Geophys. Res. Space Physics*, *118*, 393–404, doi:10.1029/2012JA018197.

Desroche, M., F. Bagenal, P. A. Delamere, and N. Erkaev (2013), Conditions at the magnetopause of Saturn and implications for the solar wind interaction, *J. Geophys. Res. Space Physics*, *118*, 3087–3095, doi:10.1002/jgra.50294.

Dougherty, M., et al. (2004), The Cassini magnetic field investigation, *Space Sci. Rev.*, *114*(1–4), 331–383, doi:10.1007/s11214-004-1432-2.

Faganello, M., F. Califano, F. Pegoraro, T. Andreussi, and S. Benkadda (2012), Magnetic reconnection and Kelvin-Helmholtz instabilities at the Earth's magnetopause, *Plasma Phys. Controlled Fusion*, *54*(12), 124037, doi:10.1088/0741-3335/54/12/124037.

Fairfield, D. H., A. Otto, T. Mukai, S. Kokubun, R. P. Lepping, J. T. Steinberg, A. J. Lazarus, and T. Yamamoto (2000), Geotail observations of the Kelvin-Helmholtz instability at the equatorial magnetotail boundary for parallel northward fields, *J. Geophys. Res.*, *105*, 21,159–21,174, doi:10.1029/1999JA000316.

Fukazawa, K., S. Ogi, T. Ogino, and R. J. Walker (2007a), Magnetospheric convection at Saturn as a function of IMF B_z, *Geophys. Res. Lett.*, *34*, L01105, doi:10.1029/2006GL028373.

Fukazawa, K., T. Ogino, and R. J. Walker (2007b), Vortex-associated reconnection for northward IMF in the Kronian magnetosphere, *Geophys. Res. Lett.*, *34*, L23201, doi:10.1029/2007GL031784.

Fuselier, S. A., R. Frahm, W. S. Lewis, A. Masters, J. Mukherjee, S. M. Petrinec, and I. J. Sillanpaa (2014), The location of magnetic reconnection at Saturn's magnetopause: A comparison with Earth, *J. Geophys. Res. Space Physics*, *119*, 2563–2578, doi:10.1002/2013JA019684.

Hwang, K.-J., M. L. Goldstein, M. M. Kuznetsova, Y. Wang, A. F. Viñas, and D. G. Sibeck (2012), The first in situ observation of Kelvin-Helmholtz waves at high-latitude magnetopause during strongly dawnward interplanetary magnetic field conditions, *J. Geophys. Res.*, *117*, A08233, doi:10.1029/2011JA017256.

Johnson, J. R., S. Wing, and P. A. Delamere (2014), Kelvin Helmholtz instability in planetary magnetospheres, *Space Sci. Rev.*, *184*, 1–31, doi:10.1007/s11214-014-0085-z.

Kanani, S. J., et al. (2010), A new form of Saturn's magnetopause using a dynamic pressure balance model, based on in situ, multi-instrument Cassini measurements, *J. Geophys. Res.*, *115*, A06207, doi:10.1029/2009JA014262.

Karimabadi, H., et al. (2013), Coherent structures, intermittent turbulence, and dissipation in high-temperature plasmas, *Phys. Plasmas*, *20*(1), 012303, doi:10.1063/1.4773205.

Lai, H. R., H. Y. Wei, C. T. Russell, C. S. Arridge, and M. K. Dougherty (2012), Reconnection at the magnetopause of Saturn: Perspective from FTE occurrence and magnetosphere size, *J. Geophys. Res.*, *117*, A05222, doi:10.1029/2011JA017263.

Ma, X., A. Otto, and P. A. Delamere (2014a), Interaction of magnetic reconnection and Kelvin-Helmholtz modes for large magnetic shear: 1. Kelvin-Helmholtz trigger, *J. Geophys. Res. Space Physics*, *119*, 781–797, doi:10.1002/2013JA019224.

Ma, X., A. Otto, and P. A. Delamere (2014b), Interaction of magnetic reconnection and Kelvin-Helmholtz modes for large magnetic shear: 2. Reconnection trigger, *J. Geophys. Res. Space Physics*, *119*, 808–820, doi:10.1002/2013JA019225.

Masters, A., N. Achilleos, C. Bertucci, M. K. Dougherty, S. J. Kanani, C. S. Arridge, H. J. McAndrews, and A. J. Coates (2009), Surface waves on Saturn's dawn flank magnetopause driven by the Kelvin-Helmholtz instability, *Planet. Space Sci.*, *57*, 1769–1778, doi:10.1016/j.pss.2009.02.010.

Masters, A., et al. (2010), Cassini observations of a Kelvin-Helmholtz vortex in Saturn's outer magnetosphere, *J. Geophys. Res.*, *115*, A07225, doi:10.1029/2010JA015351.

Masters, A., N. Achilleos, J. C. Cutler, A. J. Coates, M. K. Dougherty, and G. H. Jones (2012a), Surface waves on Saturn's magnetopause, *Planet. Space Sci.*, *65*, 109–121, doi:10.1016/j.pss.2012.02.007.

Masters, A., et al. (2012b), The importance of plasma β conditions for magnetic reconnection at Saturn's magnetopause, *Geophys. Res. Lett.*, *39*, L08103, doi:10.1029/2012GL051372.

McAndrews, H. J., C. J. Owen, M. F. Thomsen, B. Lavraud, A. J. Coates, M. K. Dougherty, and D. T. Young (2008), Evidence for reconnection at Saturn's magnetopause, *J. Geophys. Res.*, *113*, A04210, doi:10.1029/2007JA012581.

Miura, A., and P. L. Pritchett (1982), Nonlocal stability analysis of the MHD Kelvin-Helmholtz instability in a compressible plasma, *J. Geophys. Res.*, *87*, 7431–7444, doi:10.1029/JA087iA09p07431.

Nykyri, K., A. Otto, B. Lavraud, C. Mouikis, L. M. Kistler, A. Balogh, and H. Rème (2006), Cluster observations of reconnection due to the Kelvin-Helmholtz instability at the dawnside magnetospheric flank, *Ann. Geophys.*, *24*, 2619–2643, doi:10.5194/angeo-24-2619-2006.

Otto, A. (1990), 3D resistive MHD computations of magnetospheric physics, *Comput. Phys. Commun.*, *59*, 185–195, doi:10.1016/0010-4655(90)90168-Z.

Otto, A. (2001), Geospace Environment Modeling (GEM) magnetic reconnection challenge: MHD and Hall MHD-constant and current dependent resistivity models, *J. Geophys. Res.*, *106*, 3751–3758, doi:10.1029/1999JA001005.

Otto, A., and D. H. Fairfield (2000), Kelvin-Helmholtz instability at the magnetotail boundary: MHD simulation and comparison with Geotail observations, *J. Geophys. Res.*, *105*, 21,175–21,190, doi:10.1029/1999JA000312.

Parker, E. N. (1965), Dynamical theory of the solar wind, *Space Sci. Rev.*, *4*, 666–708, doi:10.1007/BF00216273.

Radioti, A., D. Grodent, J.-C. Gérard, S. E. Milan, B. Bonfond, J. Gustin, and W. Pryor (2011), Bifurcations of the main auroral ring at Saturn: Ionospheric signatures of consecutive reconnection events at the magnetopause, *J. Geophys. Res.*, *116*, A11209, doi:10.1029/2011JA016661.

Radioti, A., D. Grodent, J.-C. Gérard, B. Bonfond, J. Gustin, W. Pryor, J. M. Jasinski, and C. S. Arridge (2013), Auroral signatures of multiple magnetopause reconnection at Saturn, *Geophys. Res. Lett.*, *40*, 4498–4502, doi:10.1002/grl.50889.

Siscoe, G. L., L. Davis Jr., P. J. Coleman Jr., E. J. Smith, and D. E. Jones (1968), Power spectra and discontinuities of the interplanetary magnetic field: Mariner 4, *J. Geophys. Res.*, *73*, 61–82, doi:10.1029/JA073i001p00061.

Slavin, J. A., et al. (2008), Mercury's magnetosphere after MESSENGER's first flyby, *Science*, *321*, 85–89, doi:10.1126/science.1159040.

Sonnerup, B. U. O., and L. J. Cahill Jr. (1967), Magnetopause structure and attitude from Explorer 12 observations, *J. Geophys. Res.*, *72*, 171–183, doi:10.1029/JZ072i001p00171.

Sonnerup, B. U. Ö., and L. J. Cahill Jr. (1968), Explorer 12 observations of the magnetopause current layer, *J. Geophys. Res.*, *73*, 1757–1770, doi:10.1029/JA073i005p01757.

Terada, N., S. Machida, and H. Shinagawa (2002), Global hybrid simulation of the Kelvin-Helmholtz instability at the Venus ionopause, *J. Geophys. Res.*, *107*(A12), 1471, doi:10.1029/2001JA009224.

Terada, N., H. Shinagawa, and S. Machida (2004), Global hybrid model of the solar wind interaction with the Venus ionosphere: Ion escape processes, *Adv. Space Res.*, *33*, 161–166, doi:10.1016/j.asr.2003.05.011.

Walker, R. J., K. Fukazawa, T. Ogino, and D. Morozoff (2011), A simulation study of Kelvin-Helmholtz waves at Saturn's magnetopause, *J. Geophys. Res.*, *116*, A03203, doi:10.1029/2010JA015905.

Wilson, R. J., P. A. Delamere, F. Bagenal, and A. Masters (2012), Kelvin-Helmholtz instability at Saturn's magnetopause: Cassini ion data analysis, *J. Geophys. Res.*, *117*, A03212, doi:10.1029/2011JA016723.